Initial stage of localized corrosion in artificial pits formed with photon rupture on Zn-5 mass% Al alloy-coated steel

Masatoshi Sakairi*, Yoshiyuki Uchida[1] and Hideaki Takahashi

Graduate School of Engineering, Hokkaido University, Kita-13, Nishi-8, Kita-ku, Sapporo, 060-8628, Japan.

*Corresponding author. Tel: +81-11-706-7111, Fax: +81-11-706-7881

E-mail address: msakairi@ eng.hokudai.ac.jp

[1]Present address: Nagoya Aerospace Systems, Mitsubishi Heavy Industries, LTD., 10, Oye-cho, Minato-ku, Nagoya, 455-8515, Japan.

Abstract

The photon rupture method, by which oxide film and metal are removed by focused pulsed Nd - YAG laser beam irradiation, was applied to form artificial micro pits in Zn -5 mass% Al alloy-coated steel. The zinc alloy-coated layer was removed by pulsed laser irradiation treatment for about one second in a neutral buffer solution with NaCl. The rest potential transient with the laser treatment was measured. In the early stage of the laser treatment the rest potential of zinc alloy-coated steel changed to the negative direction immediately after every irradiation of a laser pulse and then returned to the previous value. However, after the steel substrate was exposed to the solution, the rest potential moved to the positive direction immediately after every irradiation of a laser pulse and then returned to the previous value. The amplitude and duration of the potential change after the laser irradiation increased with repetition of laser irradiation, related to the pit depth and the exposed area ratio of coated layer/steel substrate. The rest potential fluctuation difference can be explained by galvanic reaction change in the artificial pit formed by laser irradiation on the Zn alloy coated
steel.

Key words : A; Zn - 5 mass %Al alloy coated steel, B; Rest potential, C; localized corrosion, Repassivation

1. Introduction

Zinc alloy-coated steels are widely used due to their excellent corrosion protection characteristics in environments. The corrosion protection of the zinc alloy-coated layer is ascribed to the cathodic protection by a galvanic reaction between the coated layer and substrate[1 - 2], and to the formation of stable and compact corrosion products which have high corrosion resistance. Zinc ions also play an important role in corrosion resistance [3].

The examination of abrupt destruction of passive oxide films and their repair is important for a better understanding of the localized corrosion of metals. Analysis of this behavior has been carried out by monitoring potential- and current- transients after mechanical stripping of oxide films[4 - 8]. The mechanical film stripping, however, poses problems of slow film stripping, contamination from the stripping tool, and stress and strain on the substrate. Recently, there are reports of film stripping by a photon rupture method (focused pulsed Nd-YAG-laser irradiation), which solves the many of the problems caused by mechanical film stripping. The irradiation with a pulsed laser beam is able to strip oxide film at extremely high rates without contamination from the film removing tool. This technique has been applied to iron by Oltra et al. [9] and by Itagaki et al. [10], to aluminum by Takahashi et al. [11], and to zinc- and zinc-aluminum alloy-coated steel by Sakairi et al. [12 - 20].

This technique has also been applied to form micro patterns on metals. Kikuchi et al. has reported fabrication of 2 dimensional or 3 dimensional metal or organic structures [21, 22] by using laser irradiation and electrochemistry. Sakairi et al. in studying the behavior of artificial pits formed by photon rupture on zinc- or zinc alloy-coated steels has reported that the direction of the rest potential shift was affected by the area ratio of zinc or zinc - 55 mass% aluminum to steel in artificial pits [23, 24]. Immediately after laser irradiation, the rest potential shifted to the negative direction while the coated layer was exposed to the solution. However, after the steel substrate was exposed to the solution, the rest potential shifted to the positive direction immediately after laser irradiation.

The objectives of this study are to form artificial pit in the zinc-5 mass % aluminum alloy-coated steel, and to investigate the effect of the area ratio of the zinc alloy-coated layer to the steel substrate in an artificial pit of zinc - 5 mass% aluminum alloy-coated steel subjected to photon rupture, on rest potential change direction in 0.5

kmol m^{-3} H_3BO_3 - 0.05 kmol m^{-3} $Na_2B_4O_7$ (pH = 7.4) with 0.01 kmol m^{-3} NaCl.

2. Experimental

2.1 Specimen

The Zn - 5 mass% Al alloy-coated steel sheets (coated layer thickness of about 15 μm, Nippon Steel Co.) were cut into 15 x 20 mm coupons. After ultrasonic cleaning, samples were dipped in a nitrocellulose / ethyl acetate solution two times to form an approximately 30 μm thick protective nitrocellulose film on the samples.

2.2 Electrochemical measurements

After formation of the nitrocellulose film, the specimens were immersed in 0.5 kmol m^{-3} H_3BO_3 - 0.05 kmol m^{-3} $Na_2B_4O_7$ (pH = 7.4) with 0.01 kmol m^{-3} NaCl, and irradiated by a pulsed Nd - YAG laser (Sepctra Physics GCR - 130) through a lens and a quartz window at open circuit condition. The laser beam was the second harmonic wave of wave length 532 nm, wave duration 8 ns, and frequency 10 s^{-1}, and the laser power was adjusted to 30 mW in front of the lens. The irradiation interval was 0.1 s. The rest potential transient of the specimens after the laser irradiation was measured by a computer through an A/D converter. The laser irradiation time was also detected by a photo-detector.

A saturated Ag/AgCl electrode was used as a reference electrode to measure the electrochemical data.

2.3 Surface observation

After the tests, the specimen surfaces were examined by a con-focal scanning laser microscope (CSLM, Laser Tech. co.) The artificial pit depth was measured by the depth analysis function of the CSLM.

3. Results

3.1 Formation of the artificial pits

Fig. 1 shows CSLM contrast images after different periods, t_i = 0.1 and 10 s, of the laser treatment. In Fig. 1, in addition to the central dark area of about 140 μm in

diameter where high energy density beam was irradiated, in its periphery of about 300 μm in diameter the nitrocellulose film is removed by one pulse, t_i = 0.1s, of laser irradiation. Because of the thickness difference between the nitrocellulose film remaining area and the nitrocellulose film removed area, the border looks dark ring. The shape and the size of the central dark area and nitrocellulose film removed area at t_i = 0.1 s are almost the same as those at t_i = 10 s. There are no traces of thickness decrease of the zinc alloy layer in the periphery of the pit opening where the nitrocellulose film is removed by the laser treatment. It can, therefore, be said that in the area of about 300 μm in diameter only the nitrocellulose film was removed by heat influence of irradiation of a laser pulse without removing zinc alloy coating by repeated laser irradiation, whereas the central area of 140 μm in diameter was stripped off steadily with every irradiation of the central high energy density part of the pulse beam.

Fig. 2 shows the change in the pit depth with the laser treatment in 0.5 kmol m^{-3} H_3BO_3 - 0.05 kmol m^{-3} $Na_2B_4O_7$ solution. The pit becomes deeper with laser treatment time and the depth is almost the same as the thickness of Zn - 5 mass% Al alloy-coated layer after the repeated laser irradiation treatment for about 2s. The slope changes after the zinc alloy-coated layer is removed in the irradiated area because of removal efficiency difference between the zinc alloy-coated layer and steel substrate, which depends on the reflectivity and thermal property of the materials. This result suggests that the laser irradiation treatment for about 3 s is long enough to remove the zinc alloy-coated layer.

The pit diameter is about 140μm and the maximum depth of the pit is 60 μm from Figs. 1 and 2. The aspect-ratio (depth/diameter) of artificial pits is less than 0.5. On the assumption of a cylindrical pit formation, the exposed areas of coated layer and steel were calculated. The area ratio of steel substrate/zinc alloy-coated layer exposed to the solution changes from 0 to about 0.6 in this experiment. Thus, this technique enables us to make an artificial micro-pit on the zinc alloy-coated steel and to change the area ratio of zinc-aluminum alloy to steel.

The duration of laser treatment can be divided into three stages; only the zinc alloy-coated layer is exposed to the solution at Stage I, and both zinc alloy-coated layer and steel substrate are exposed to the solution at Stage III. A part of the substrate is exposed to the solution at Stage II, that is, the interval between Stages I and III. Fig. 3 is a schematic outline of cross sections at each stage.

3. 2 Rest potential change after laser irradiation

Fig. 4 shows change in the rest potential with time during repeated laser irradiation in 0.5 kmol m^{-3} H_3BO_3 - 0.05 kmol m^{-3} $Na_2B_4O_7$ with 0.01 kmol m^{-3} NaCl. Before laser irradiation, the rest potential showed a positive value because the specimen surface was covered by the nitrocellulose film. The rest potential is suddenly moved to the negative direction after one pulse of laser irradiation. During repeated laser irradiation treatment, the rest potential is moved to the positive direction with potential fluctuation, the frequency of which is the same as the pulse frequency of the laser. The potential after the laser treatment for 10 s reaches about - 1 V.

Fig. 5 shows changes in the rest potential with the laser treatment at Stages I-III in Fig. 4. Laser was irradiated at the time indicated by arrows in Fig. 5. The potential changes periodically, the interval of which is the same as the laser irradiation interval of 0.1 s. Thus the periodic potential change results from irradiation of a laser pulse. The rest potential is suddenly decreased immediately after every irradiation of a laser pulse up to a sharp minimum and then returned to the previous value at Stage I. However, the direction of rest potential shift at Stage III is opposite to that at Stage I. At Stage I, the amplitude of the rest potential fluctuation becomes smaller with repeated irradiation, related to pit depth and exposed area of metal, whereas at Stage III, the amplitude of the rest potential fluctuation becomes larger with repeated irradiation, also related to pit depth and exposed area of metal. The direction of rest potential shift changes during Stage II, because Stage II is a transitional stage between Stage I and Stage III.

4. Discussion

4.1 Formation speed of pit

The approximate expression for the minimum laser power density of ablation, E_{ab}, is $2 \cdot L \cdot p \cdot k^{0.5} \cdot t_p^{-0.5}$, where L is the latent heat required to vaporize the solid metal, p the density of the metal, k the thermal diffusibility and t_p the pulse duration [25]. The laser power density of E_{ab} for both of the zinc alloy-coated layer and the steel substrate is estimated to be about 10^{12} W / m^2. The absorbed power density of the material by one pulse of laser irradiation, E_{abs}, is expressed by $E_{abs} = 4 (1 - R) P / [\pi \cdot D^2 \cdot t_p]$, where R is the reflectance of the material, P is the mean irradiated laser power, D is the

diameter of the irradiated area, and t_p is the pulse duration. The absorbed power density can be estimated to be about 4 x 10^{12} W / m^2 in this experiment. This indicates that the artificial pit was formed by laser ablation due to formation of a gas or plasma.

Table 1 shows material constants for mild steel and zinc. The pit formation rate of zinc alloy-coated layer is about 16 μm s^{-1} and that of steel substrate is about 5 μm s^{-1}. By using table 1 and these values, it is possible to calculate the absorbed heat energy during unit time. The heat energy absorbed by zinc alloy-coated layer during laser irradiation is about 3.9 x 10^{-3} J s^{-1} and that absorbed by steel substrate is about 4.9 x 10^{-3} J s^{-1}. It is also possible to estimate the absorbed laser energy using reflectance and irradiated laser power. The reflectance of mild steel may be almost the same as iron, 0.57 at the wave length of 532 nm, and that of zinc alloy-coated layer may be almost the same as that of zinc, 0.75. The calculated energy absorbed by zinc alloy-coated layer is about 7.5 x 10^{-3} J s^{-1} and that of steel substrate is about 1.3 x 10^{-2} J s^{-1}. In both materials, the absorbed laser energy is calculated by using reflectance, and the irradiated laser power is lager than that calculated by using pit formation rate and material constants. This disagreement may be due to inaccuracy or lack of reflectance and material constants. Nevertheless this simple calculation indicates that the irradiated laser energy is high enough to produce the gas-causing laser ablation.

4.2 Potential fluctuations

Fig. 6 shows a schematic outline of the anodic and cathodic polarization curves. Solid lines are those before laser irradiation, and dotted lines are the anodic polarization curve immediately after irradiation of a laser pulse at Stage I and the cathodic polarization curve immediately after irradiation of a laser pulse at Stage III. In this study, the anodic and cathodic reactions are as follows

$$\left.\begin{array}{l} Zn \rightarrow Zn^{2+} + 2e^- \text{ (main reaction)} \\ Al \rightarrow Al^{3+} + 3e^- \end{array}\right\} \quad \text{Anodic reactions}$$

$$O_2 + 2H_2O + 4e^- \rightarrow 4OH^- \quad \text{Cathodic reaction}$$

Irradiation of a pulse of laser beam results in the change in the anodic and cathodic sites. At Stage I, irradiation of a laser pulse leads to direct exposure of fresh surface of

zinc alloy to the solution. This is responsible for a sudden shift of the rest potential to the negative direction due to accelerated dissolution of the fresh surface without appreciable change in the cathode area of the rest of the Zn alloy surface exposed to the solution. However, anodic dissolution of zinc and aluminum gives rise to the rapid formation of their hydroxides. This brings about suppression of anodic dissolution with a consequent return of the rest potential to the previous value before laser irradiation.

After complete removal of zinc alloy layer by laser irradiation such as at Stage III, the direct exposure of fresh steel surface to the solution immediately after irradiation of a laser pulse results in active oxygen reduction on the fresh steel surface, whereas the anodic dissolution occurs at the periphery of the pit where hydroxides-covered zinc alloy is exposed to the solution. This leads to the rest potential shift toward positive direction. The cathodic reaction induces alkalization of the solution just above cathodically active steel surface even in the buffer solution. Because of the pH increase, the activated steel surface may be covered by zinc and aluminum hydroxides. Thus the cathodic activity of the steel surface is readily suppressed and the rest potential returns to the previous value before laser irradiation.

It has been revealed from this type of studies that the photon rupture method will be able to form an artificial pit of controlled size and aspect ratio *in situ* in the solution and enable us to study various pitting corrosion phenomena including the locations and roles of anodic and cathodic reactions in the pitting corrosion, the characteristics of solutions such as concentration and pH change inside and outside of pit, pit growth and re-passivation.

4. Conclusions

The effect of the area ratio of the zinc alloy-coated layer to the steel substrate in artificial pits, formed by photon rupture in zinc- 5 mass% aluminum alloy-coated steel, on rest-potential change direction was examined, and the following conclusions may be drawn.

1) An artificial micro pit was formed in a zinc- 5 mass% aluminum alloy-coated steel by repeated irradiation of focused pulsed YAG laser. The pit diameter remained constant

and the depth increased with repeated irradiation. The pit formation speed in the zinc alloy-coated layer was higher than that in the steel substrate.

2) Immediately after laser irradiation, the rest potential was shifted to the negative direction due to accelerated dissolution of the fresh surface of the zinc- 5 mass% aluminum alloy layer exposed directly to the solution. This situation is ended shortly owing to formation of zinc and aluminum hydroxides covering the active anode site.

3) After complete removal of the Zn alloy layer by laser irradiation direct exposure of the fresh surface of the steel substrate to the solution results in the shift of the rest potential to the positive direction because of active cathodic reaction on the fresh steel surface. This situation is ended in a short time due to formation of corrosion products of zinc and aluminum on the cathodically active surface.

Acknowledgements

The authors are indebted to The Iron and Steel Institute of Japan for financial support and thank Nippon Steel Co. for providing the zinc - 5 mass% aluminum alloy coated steel sheets.

REFERENCES

[1] Y. Hisamatsu, *Bull. Jpn. Instl. Mtals*, **20** (1981) 3.
[2] Y. Miyoshi, J. Oka and S. Maeda, *Trans ISIJ*, **23** (1983) 974.
[3] ISIJ: Research report for fundamentals of corrosion protection and evaluation methods on zinc and zinc alloy coated steels, Tokyo (2005).
[4] F. P. Ford, G. T. Burstein, and T.P. Hoar, *J. Electrochem. Soc.*, **127** (1980) 1325.
[5] G. T. Burstein and P. I. Marshall, *Corros. Sci.*, **23** (1983) 125.
[6] G.T. Burstein and R. C. Newman, *Corros. Sci.*, **21** (1981) 119.
[7] G.T. Burstein and R. J. Cinderey, *Corros. Sci.*, **32** (1991) 1195.
[8] R. J. Cindery and G. T. Burnstein, *Corros. Sc.*, **33** (1992) 493.
[9] R. Oltra, G. M. Indrianjafy and R. Roberge, *J. Electrochem. Soc.*, **140** (1993) 343.

[10] M. Itagaki, R. Oltra, B. Vuillemin, M. Keddam, and H. Takenouti, *J. Electrochem. Soc.*, **144** (1997) 64.

[11] M. Sakairi, Y. Ohira and H. Takahashi, *Electrochem. Soc. Proc.*, **97-26** (1997) 643.

[12] M. Sakairi, K. Itabashi and H. Takahashi, *Corros. Sci. and Tech.*, **31** (2002) 426.

[13] M. Sakairi, K. Itabashi and H. Takahashi, *Proc. of Japan-China Joint Seminar on Marin Corrosion* (2002) 58.

[14] M. Sakairi, K. Itabashi and H. Takahashi, *Electrochem. Soc. Proc.*, **2002-24** (2002) 399.

[15] M. Sakairi, K. Itabashi and H. Takahashi, *Proc. of Int. Symposium Corrosion Science in the 21st Century* (2003) C093.

[16] M. Sakairi, K. Itabashi and H. Takahashi, *Zaiyro-to-Kankyo*, **52** (2003) 524.

[17] M. Sakairi, K. Itabashi and H. Takahashi, *Proc. of 13th APCCC* (2003) 62.

[18] M. Sakairi, K. Itabashi and H. Takahashi, *ISIJ Int.*, **45** (2005) 71.

[19] M. Sakairi, K. Itabashi, Y. Uchida and H. Takahashi, *Corros. Sci.*, **47** (2005) 2461.

[20] M. Sakairi, K. Itabashi, Y. Uchida and H. Takahashi, T*etus-to-Hagane*, **92** (2006) 16.

[21] T. Kikuchi, M. Sakairi and H. Takahashi, *J. Electrochem. Soc.*, **150** (2003) C567.

[22] T. Kikuchi, M. Sakairi, H. Takahashi, Y. Abe, and N. Katayama, *Surface and coatings technology*, **169 - 170** (2003) 199.

[23] M. Sakairi, Y. Uchida, H. Takahashi, "Passivation of Metals and Semiconductors, and Properties of Thin Oxide Layers", Edited by P. Marcus and V. Maurice Elsevier (2006) 561.

[24] M. Sakairi, Y. Uchida, H. Takahashi, *ISIJ Int.*, **46** (2006) 1218.

[25] C. B. Scruby and L. El Drain, Laser Ultrasonics - Techniques and Applications - , Adam Hilger, New York (1990) 243.

Captions

Table 1 Material constants for mild steel and zinc.

Fig. 1 CSLM contrast images after pulsed laser irradiation treatment for 0.1 and 10 s.

Fig. 2 Change in the artificial pit depth with laser treatment time in 0.5 kmol m^{-3} H_3BO_3 - 0.05 kmol m^{-3} $Na_2B_4O_7$ with 0.01 kmol m^{-3} NaCl.

Fig. 3 Schematic outline of cross sections of each stage with increasing repetition of pulsed laser irradiation.

Fig. 4 Change in the rest potential with time during repeated pulsed laser irradiation in 0.5 kmol m^{-3} H_3BO_3 - 0.05 kmol m^{-3} $Na_2B_4O_7$ with 0.01 kmol m^{-3} NaCl.

Fig. 5 Typical examples of change in the rest potential with irradiation of two laser pulses at Stages I-III in Fig. 4. The arrows indicate the time when laser irradiation was carried out.

Fig. 6 Schematic outline of polarization curves before and immediately after irradiation of a laser pulse at Stages I and III.

Table 1

	Mild steel [25]	Zinc
Thermal capacity	480 J kg^{-1} K^{-1}(at 298K)	388 J kg^{-1} K^{-1}(at 298K)
Thermal capacity	670 J kg^{-1} K^{-1}(at 773K)	480 J kg^{-1} K^{-1}(at 495K)
Thermal capacity liquid	824 J kg^{-1} K^{-1}	479 J kg^{-1} K^{-1}
Latent heat of fusion	247 J kg^{-1}	112 J kg^{-1}
Melting point	1810 K	693 K
Boiling point	3030 K	1180 K
Latent heat of vaporization	6258000 J kg^{-1}	1755620 J kg^{-1}
Density	7900 kg m^{-3}	7134 kgm^{-3}

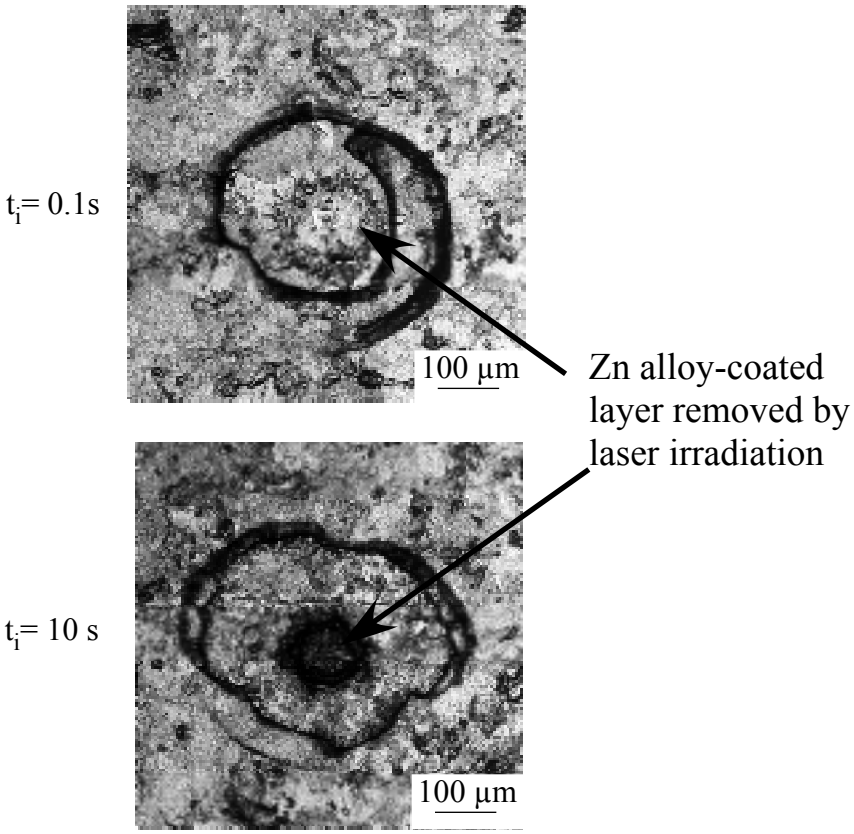

Fig. 1 Sakairi et al.

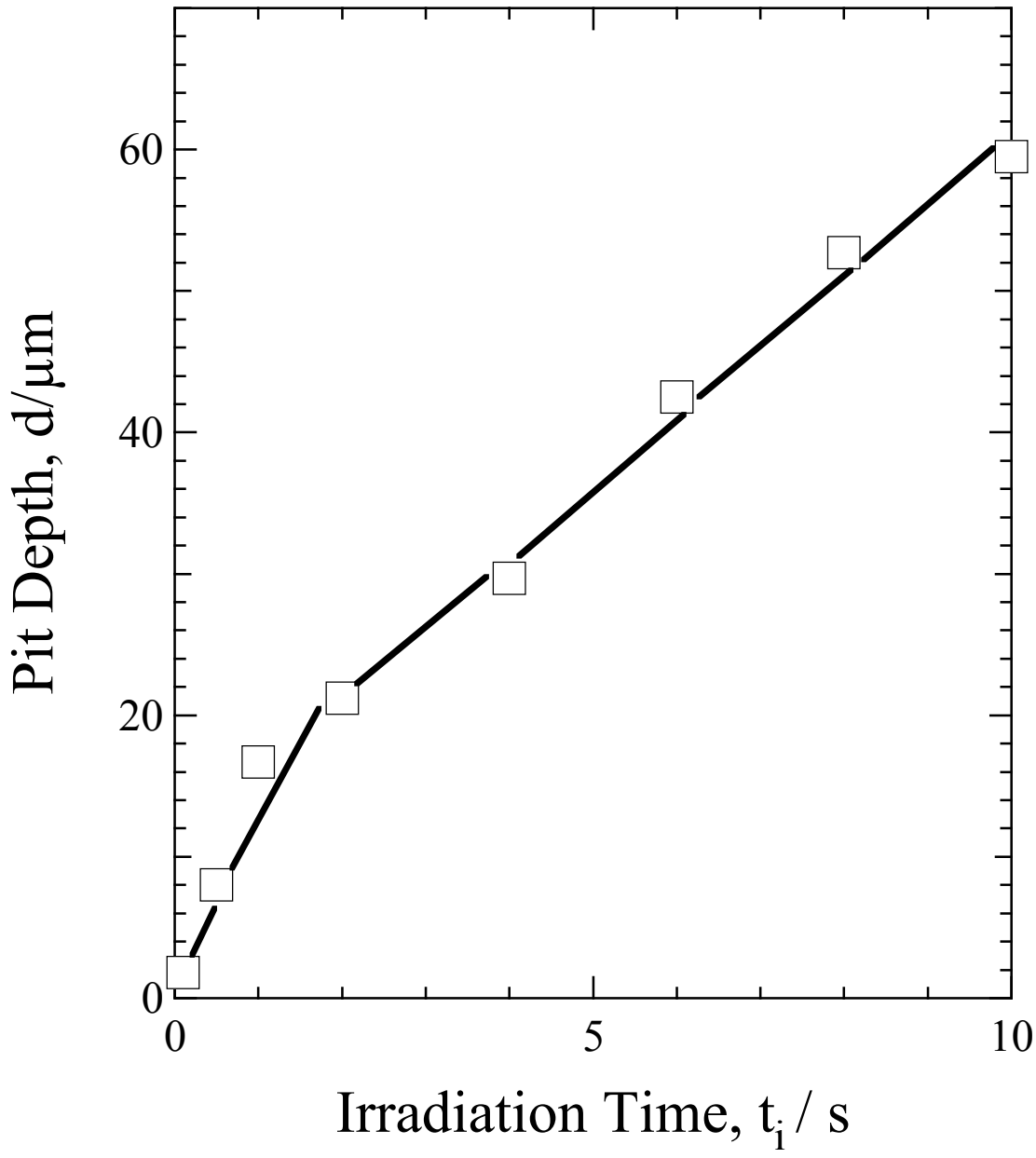

Fig. 2

Sakairi et al.

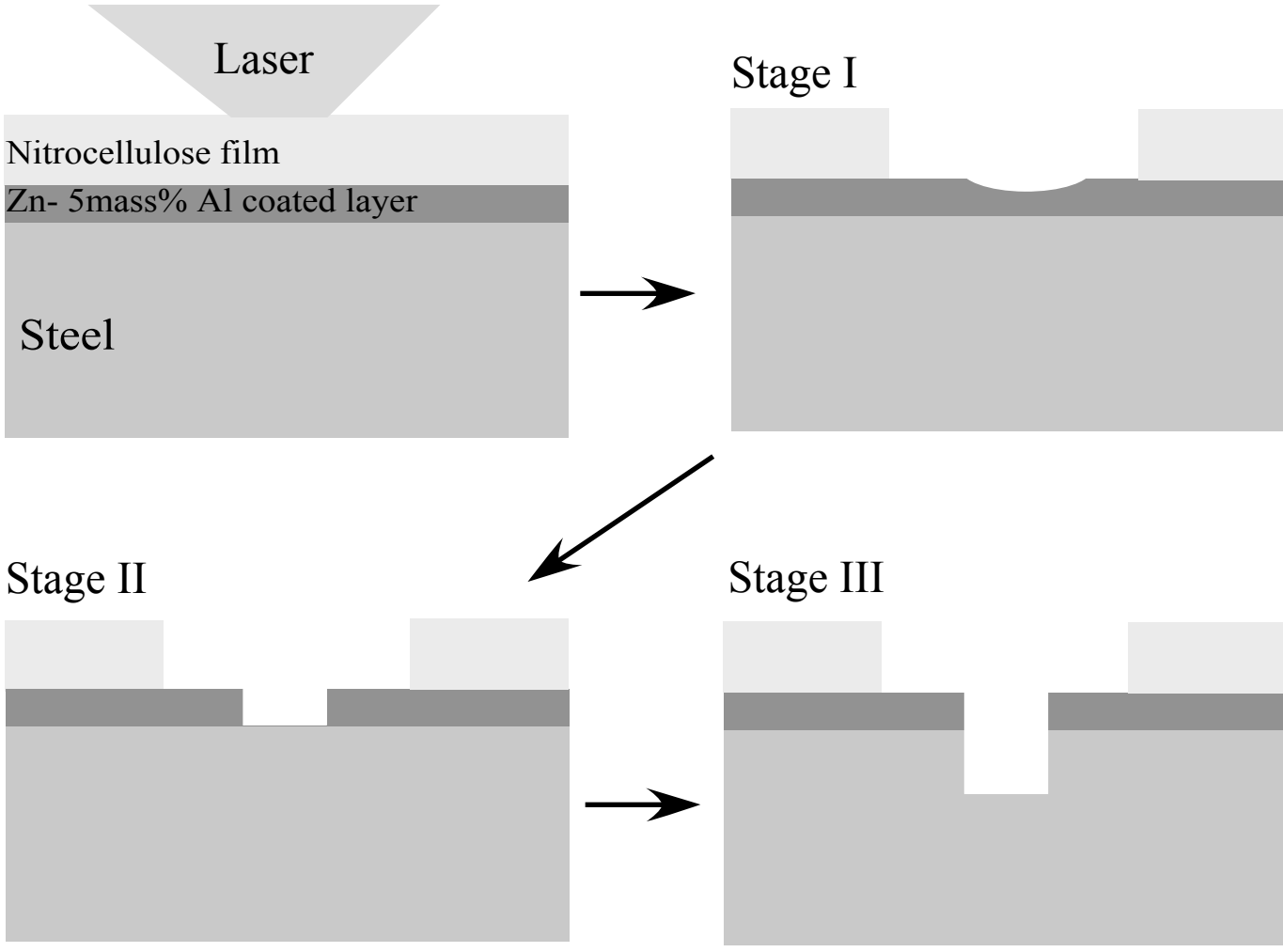

Fig. 3

Sakairi et al.

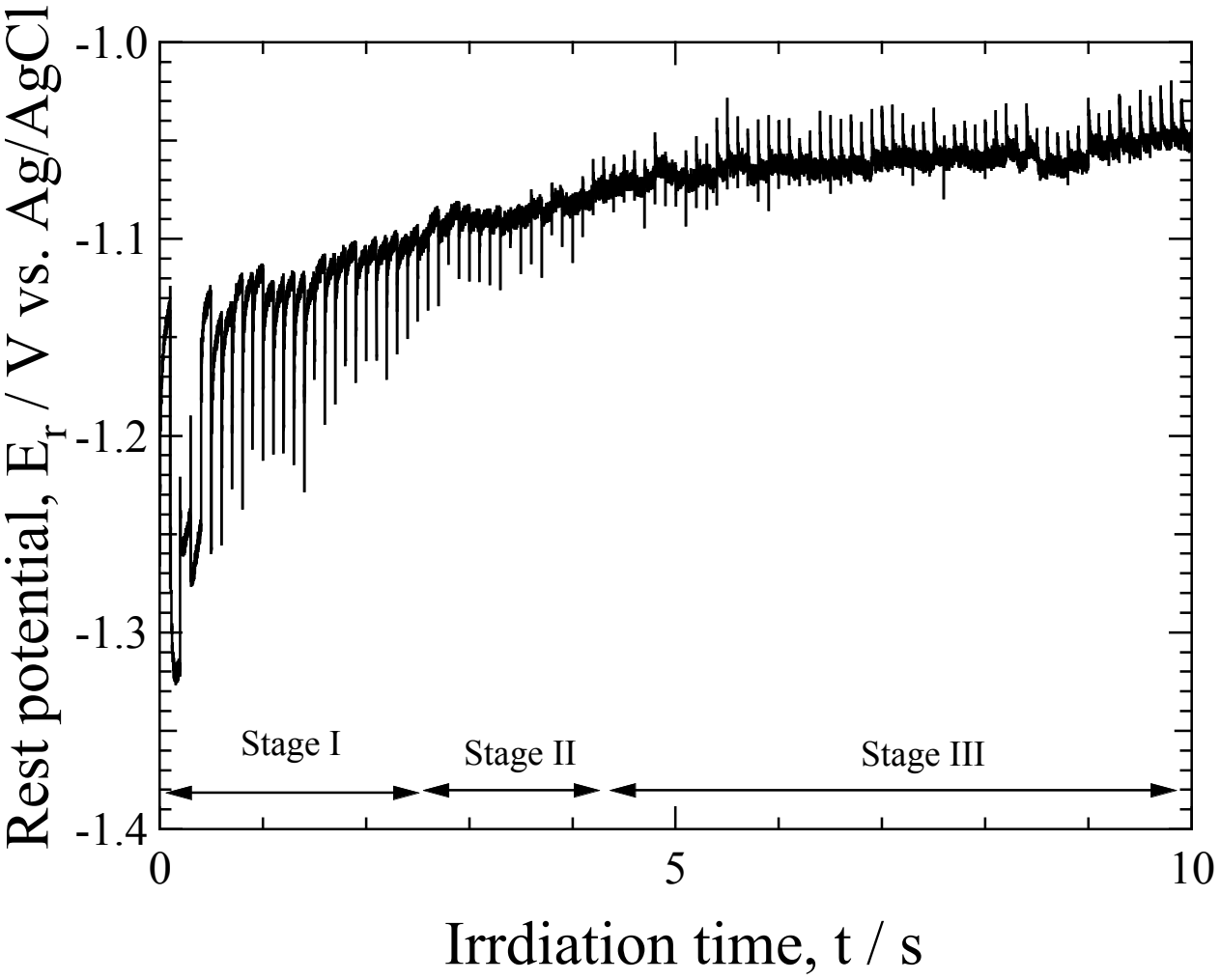

Fig. 4

Sakairi et al.

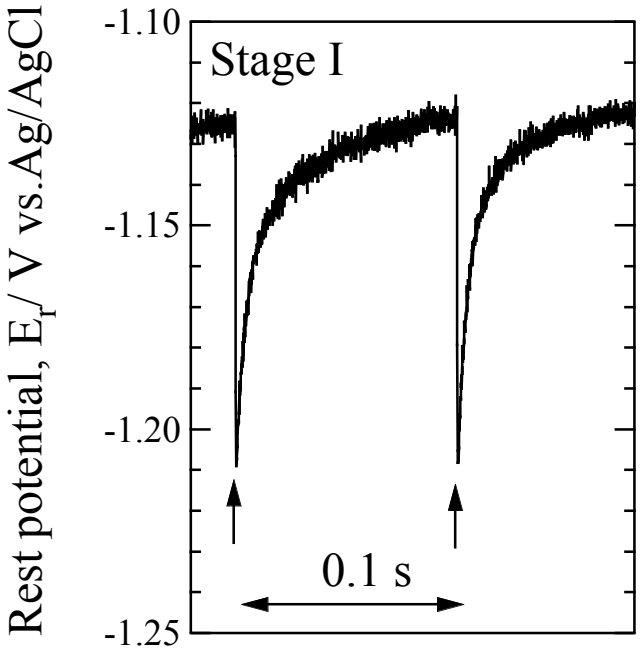

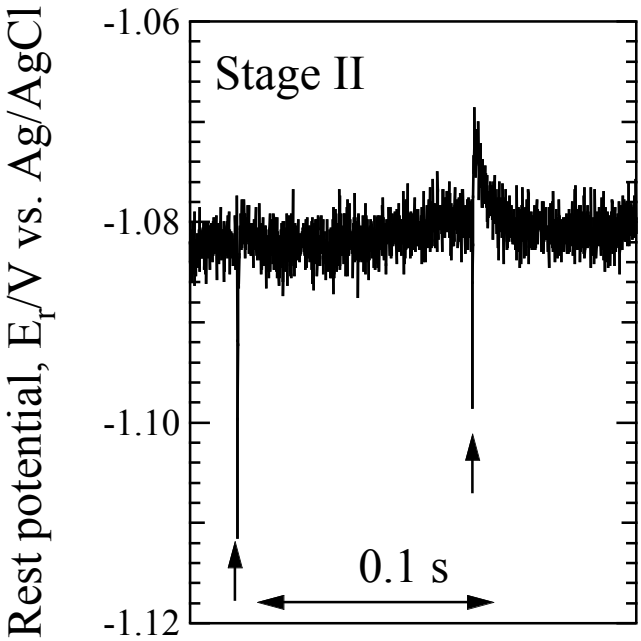

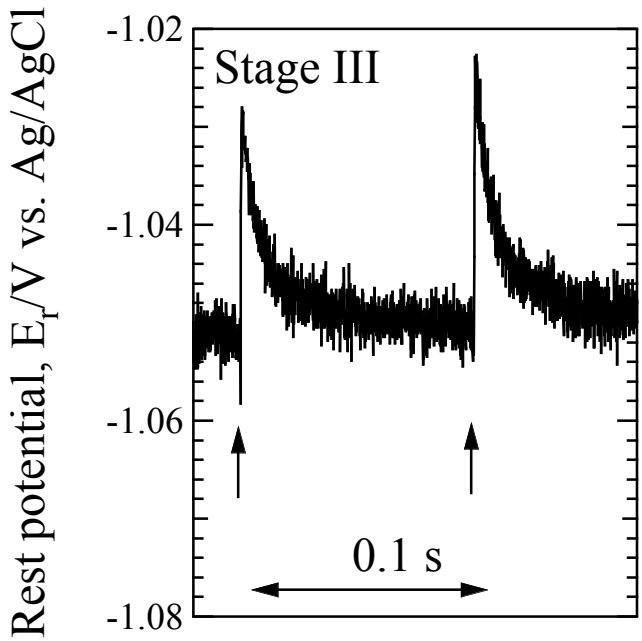

Fig.5

Sakairi et al

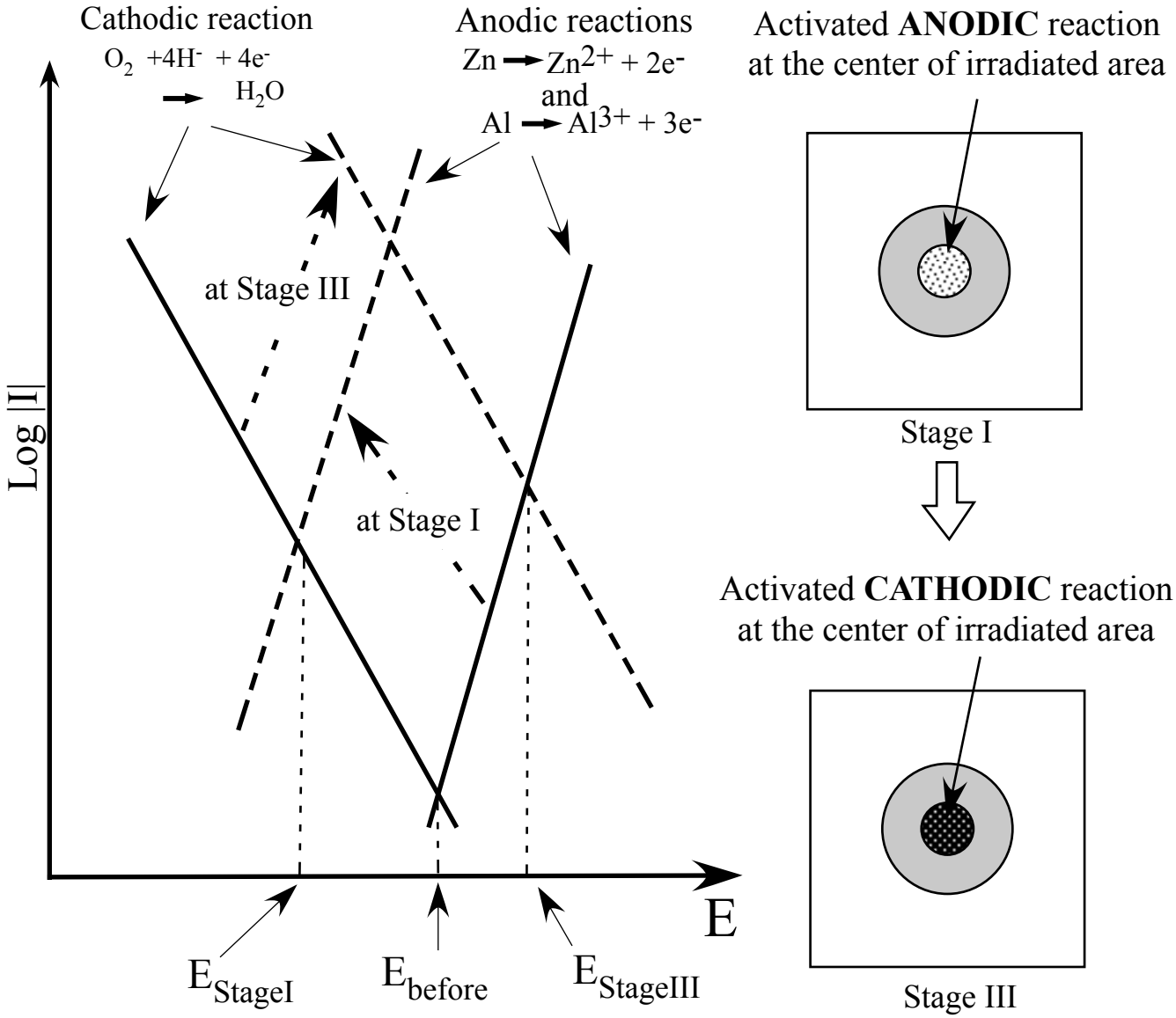

Fig. 6

Sakairi et al.